

Silver Nanodisk Growth by Surface Plasmon Enhanced Photoreduction of Adsorbed $[\text{Ag}^+]$

Mathieu Maillard, Pinray Huang,[†] and Louis Brus*

Chemistry Department, Columbia University, New York, New York 10027

Received August 16, 2003; Revised Manuscript Received September 18, 2003

ABSTRACT

The photoreduction of silver ions by citrate, catalyzed on silver seeds, is used to synthesize disk-shaped silver nanoparticles in solution. The reaction is characterized by transmission electron microscopy (TEM), atomic force microscopy (AFM), optical absorption spectroscopy, and by measuring the silver ion concentration during the reaction. The irradiation wavelength determines the final shape of these particles due to the shape dependence of the Ag plasmon spectrum. The quantum yield of this reaction has been calculated, and a growth mechanism is outlined.

Introduction. Silver particles provide an ideal system for study of size and shape effects in the surface plasmon resonance; indeed, this sensitivity is a tool to monitor the shape of the particles during their synthesis via the optical extinction spectrum. Plasmon resonances concentrate an incident electromagnetic field via near-field enhancement; this antenna effect is the source of surface enhanced Raman scattering (SERS). The intense Ag resonance allows single molecule observation in SERS,^{1–5} enables coupled Ag particles to form a subwavelength waveguide,⁶ and enables sensitive colorimetric DNA screening.^{7,8}

Henglein^{9,10} has shown that the physical and chemical properties of finely divided, nm-sized Ag particles are strongly modified by the adsorption of nucleophilic species and that Ag particles catalyze thermal and optical electrochemical reactions. For example, core/shell metallic particles can be grown.¹¹ Indeed, adsorption of chemical species modifies the Fermi level of both the metal and the reactant, like a polarized nanoelectrode.

Combining these effects, we now report controlled photochemical Ag particle growth from adsorbed Ag silver ions in the presence of citrate. If different shapes and sizes are present in a seed colloid, the particle with the largest plasmon absorption cross-section at the laser wavelength initially grows fastest. The reaction accelerates for those shapes whose plasmons move into resonance with the photochemical wavelength as growth occurs. This effect allows control of shape in the dominant photoproduct by choice of photochemical wavelength. There have been previous observations

of reduced silver formation by irradiation of citrate and Ag ion, however, without control of shape or size.^{12,13}

Synthesis. An aqueous Ag seed colloid is synthesized by adding 0.5 mL of 25 mM ice-cold sodium borohydrate into a stirring solution of 20 mL of 10 mM citrate and 0.5 mL of 5 mM silver nitrate. This solution is stirred for 5 min and aged for 24 h. The growth solution is made by mixing 100 μL of seed colloid, 50 μL of 10 mM citrate, 50 μL of 5 mM silver nitrate, and 800 μL of ultrapure water. Hence, the silver ion and the metallic silver concentrations are 2.5×10^{-4} M and 2.5×10^{-5} M, respectively. This solution is kept refrigerated in the dark. In a typical experiment, 200 μL of this solution is uniformly irradiated at 23 °C in a 4.3 mm wide optical cell with a linearly polarized argon laser beam.

Growth and Characterization at 457 nm. TEM examination shows the seed colloid has round Ag particles of 8 nm average size. Growth solutions initially show the Ag seed resonance in the blue at 395 nm (Figure 1). Such solutions irradiated at 457 nm at 0.8 W/cm² change from pale yellow to purple within an hour. The dominant photochemical product Ag particles have a disklike or triangular shape; their average diameter, measured by TEM (Figure 2), is $D = 38$ nm. Their average height has been measured by AFM as $h = 10.7$ nm, corresponding to an aspect ratio $D/h = 3.57$, which is in a good agreement with the aspect ratio measured by TEM of the few particles standing on the short side. As observed by electron diffraction, the majority of the disks are single crystal. This flat triangular shape already has been obtained by numerous syntheses using different experimental conditions with gold¹⁴ and silver^{15–19} and seems to be related to a stacking fault constraint.²⁰ The corresponding absorption

* Corresponding author.

[†] REU student, present address New College of Florida.

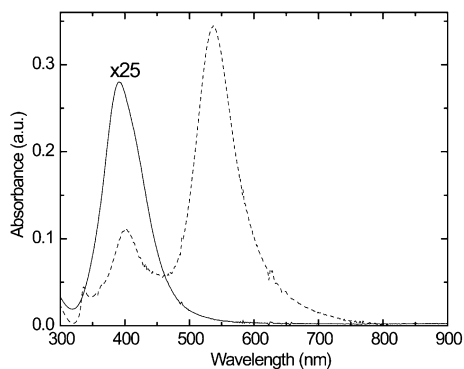


Figure 1. Plot of the absorption spectrum from a product disk solution (dashed line) and the reagent silver seed solution (solid line).

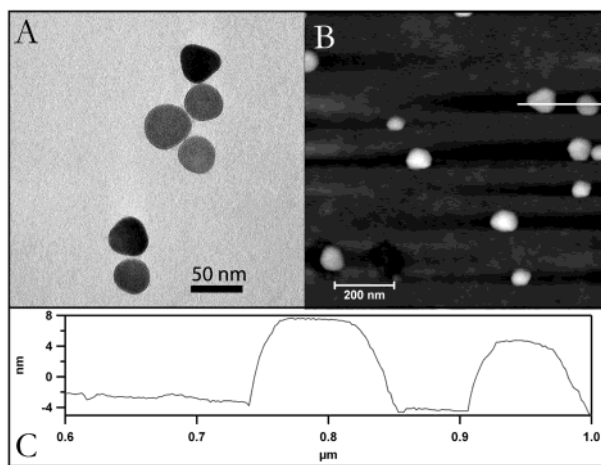


Figure 2. (A) TEM picture of the silver nanodisks after 90 min of irradiation at 0.8 W/cm² at λ = 457 nm. (B) AFM picture of product particles. (C) height profile along the line in Figure 1B.

spectrum (Figure 1) exhibits two additional peaks at 338 and 540 nm corresponding to the transverse and longitudinal plasmon modes and an increase of the initial plasmon band at 400 nm. The absorption spectrum of such a particle in water can be easily calculated assuming a flat ellipsoid shape.²¹ The calculated model exhibits two plasmon bands at 340 and 510 nm. The slight discrepancy in the long wavelength peak position is explained by the simplified shape of this model. According to calculations by Schatz et al.,¹⁷ the longitudinal plasmon mode of an exact triangular particle is, indeed, more red shifted.

The growth process has been characterized by TEM (Figure 3), by AFM, by absorption spectroscopy (Figure 4B), and by measuring the silver nitrate concentration with an ion selective electrode (Figure 4A) at different irradiation times, up to 90 min. The silver concentration initially decreases linearly as a function of time, as: $\partial[\text{Ag}^+]/\partial t = K = 2.09 \times 10^{-7} \text{ mol s}^{-1}$ which corresponds to a half-reaction time constant of 20 min. This linear behavior indicates that the reaction does not depend on the initial silver concentration in solution. The silver ions are in excess in the solution: the silver concentration on the nanoparticle surface is completely saturated and remains constant as long as the concentration is high enough. The quantum yield of this

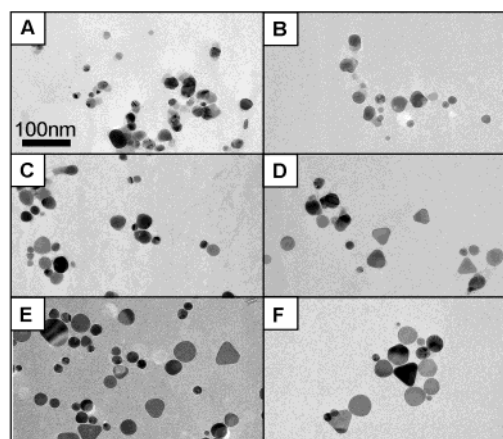


Figure 3. From A to F, TEM pictures of the particles synthesized after $t = 5, 10, 15, 20, 50,$ and 90 min of irradiation.

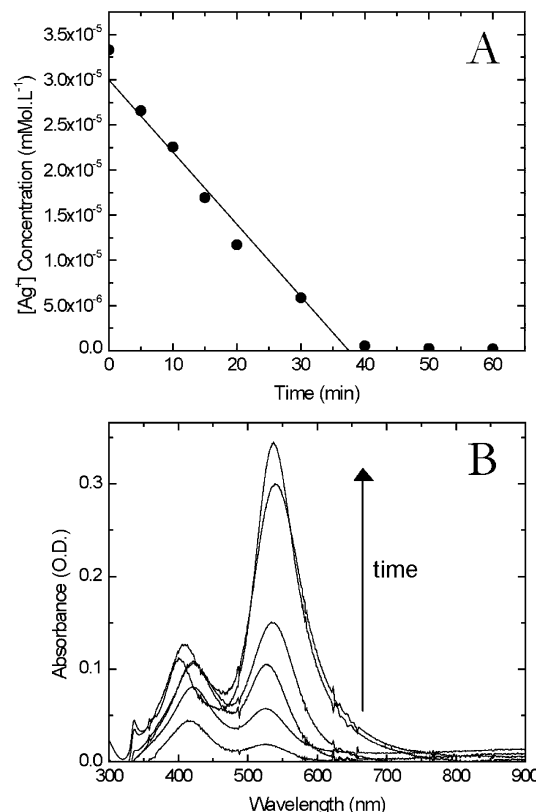


Figure 4. (A) Plot of the silver concentration (7.5 times diluted) vs the irradiation time. Solid line is a linear fit. Each point corresponds to a different diluted sample. (B) Plot of the absorption spectra after $t = 5, 10, 15, 20, 50,$ and 90 min of irradiation.

photoreaction has been calculated as

$$QY = \frac{\partial n_{\text{Ag}^+}}{\partial n_{\text{photon}}^a} = \frac{\frac{\partial n_{\text{Ag}^+}}{\partial t}}{\frac{\partial n_{\text{photon}}^a}{\partial t}} = \frac{K V h \nu (1 - 10^{-\text{D.O}})}{P} = 0.08\%$$

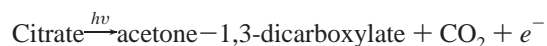
where $\partial n_{\text{Ag}^+}/\partial t = K$ is the rate of silver atoms reduction, deduced from the kinetic study, $\partial n_{\text{photon}}^a/\partial t = [V h \nu (1 - 10^{-\text{D.O}})]/P$ is the rate of photon absorption, $h \nu$ is the photon

energy, $A = 1 - 10^{-DO}$ is the absorbance,²² $DO = 0.065$ is the initial optical density of the solution, P is the laser power, and V is the irradiated volume. This low quantum yield, 0.08% per photon at saturated $[Ag^+]$ coverage, and the linear decrease are consistent with the assumption that adsorption of silver ions and citrate molecules on the nanoparticle are not the limiting factor of this reaction.

During growth, particles present a characteristic shape evolution. Starting with a spherical shape, the particles grow as spheres and then evolve into more well-defined, triangular, disklike shapes. As observed by TEM after a 5 min irradiation, the average particle size quickly increases from 8 to 14 nm as their shape remains roughly spherical. The absorption spectrum of these particles agrees with the growth, since the plasmon band at 400 nm increases in intensity from 0.006 to 0.04, while only a weak band at 530 is observed. From 10 to 20 min, (Figure 3B to 3D), the shapes of the particles become more and more well defined with the appearance of few triangular particles. At the same time, the absorption band at 400 nm is still increasing. The major effect, however, is the increase of the two plasmon bands related to the shape transformation, at 338 and 540 nm. Finally, after 50 and 90 min (Figure 3E and 3F), the particles are very similar in shape; most of them being flat particles. The number of small spheres significantly decreases, as observed by spectroscopy in the increase of the disk-related plasmon band and the decrease of the peak at 400 nm. This last peak does not completely disappear, even with a low percentage of spheres since it is also related to a weak quadrupolar plasmon mode from the flat particles.¹⁷

Several control experiments were done. The reaction does not occur on this time scale if any of the reactants (i.e., the seeds, the silver ions, or the citrate) are not present. Furthermore, this reaction is drastically slowed when the growth solution is stored in the dark; thermal reaction is much slower than photoreaction at room temperature. This experiment was also performed by varying the laser intensity and the irradiation time while keeping a constant fluence of $F = 480 \text{ J cm}^{-2}$. In the intensity range 0.16 W/cm^2 to 0.8 W/cm^2 , both the silver ion aqueous concentration and the absorption spectra were nearly identical after the corresponding irradiation time (10 to 50 min, depending on the intensity). This particular control experiment indicates that photoreduction is linear with the light intensity. From this, the hypothesis of a thermally activated mechanism due to the heating of the irradiated particles can be excluded.

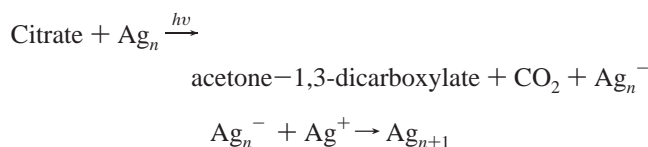
Mechanism and Change of Wavelength. Citrate molecules play a key role. Citrate acts as a capping ligand for the silver particles as well as a photoreducing agent for the silver ions. Citrate has three carboxylic groups and it has been shown by Munro et al.²³ that mainly two of them would bind to the silver surface, leaving the third one normal to the surface and responsible for the colloid stabilization by electrostatic repulsion. Citrate is known to photoreduce on colloidal silver, apparently by the process^{12,24}



Furthermore, carboxylic groups from citrate are nucleophilic

and their adsorption onto the nanoparticle surface induces a fractional electron transfer. According to Henglein's work, this effect, summed over all the adsorbed molecules, induces a displacement of the metal Fermi level toward the more negative potentials. Simultaneously, the carboxylic group redox potential increases and becomes easier to photooxidize.⁹

In addition, nanoparticles are able to act as an electron storage and transfer medium. This has been observed in the past as a displacement of the plasmon resonance after electron injection inside silver nanoparticles, and an increase of the chemical reactivity on its surface.²⁸ Hence, silver ions might more easily be reduced on the nanoparticle surface. While not proven, the reaction we observe is likely to be^{12,13,23-25}



At the beginning of the reaction, the seeds absorb light isotropically (equally for all orientations with respect to the laser polarization) due to their spherical shape. As some inhomogeneity occurs in the deposited silver layer, the particle starts to become ellipsoid-like, and the degenerate plasmon resonance splits into transverse and longitudinal modes. The longitudinal plasmon (along the longer dimension) shifts to longer wavelength, toward 457 nm, and absorbs this wavelength more strongly, on a rotationally averaged basis in solution, than the transverse mode, which shifts to shorter wavelength. If we assume that reduced atoms are deposited in proportion to the near field intensity enhancement at the surface position, then this longer axis grows preferentially. The process accelerates until the longitudinal plasmon wavelength shifts beyond the irradiation wavelength. Such anisotropic growth was apparently first observed in Cd metallic particles on surfaces grown by plasmon enhanced photodissociation of dimethylcadmium in the gas phase by Osgood et al.²⁶

Why do we observe disks rather than rods? The initial spherical plasmon is 3-fold degenerate. We suggest that the shape that grows the fastest will have the largest absorption coefficient at the irradiation wavelength when rotationally averaged; our synthesis is performed in solution and particles consequently have a random orientation compared to the incident light. In the disk, the longitudinal plasmon is doubly degenerate in the plane; in the rod it is not degenerate. Taking into account that reaction rate is related to the field enhancement and assuming a deviation angle α of the laser polarization from the optimum orientation, we can calculate the reaction solid angle for these two shapes, $W_r = 4\pi(1 - \cos\alpha)$ and $W_d = 4\pi \sin\alpha$, respectively, for a rod and a disk. The ratio $W_d/W_r = (1 - \cos\alpha)/\sin\alpha$ is always larger than 1, especially when α is small. This heuristic argument suggests that a disk has a larger rotationally averaged absorption coefficient at 457 nm than a rod. The fact that we do not see three separate peaks at intermediate time implies that

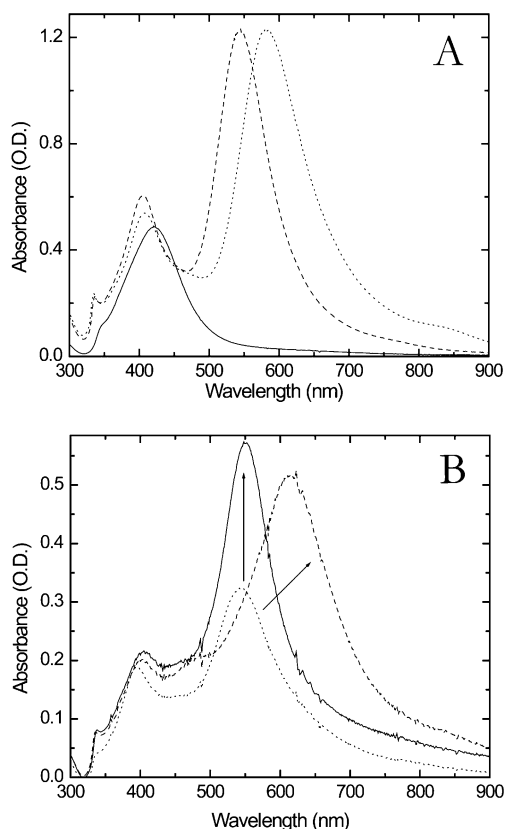


Figure 5. (A) Plot of the product absorption after irradiation at 368 (solid line), 457 (dashed line), and 514 nm (dotted line). (B) Plot of the absorption before (dotted line) and after the regrowth process at 457 (solid line) and 514 nm (dashed line).

the two in-plane dimensions grow at about same rate. This self-induced anisotropic growth mechanism stops only when the aspect ratio of the particle is large enough so that the corresponding longitudinal plasmon mode is too far in the red compared to the irradiation wavelength. Then the absorption cross-section turns to be too small and comparable to the transverse mode. The photoreduction process is then less efficient and, more importantly, no longer anisotropic. This mechanism needs to be confirmed by quantitative calculations.

This mechanism is supported by changing the irradiation wavelength from 457 to 514 nm (Figure 5A) at 0.18 W/cm^2 . The final absorption spectrum exhibits a significant red shift from 540 to 585 nm. In both cases, disks rather than rods grow.

In the case of UV irradiation, the laser is used in multiline mode between 333 and 364 nm at the same intensity, so the laser wavelength is slightly below the spherical plasmon position. If the particle aspect ratio increases, the new plasmon mode in the UV corresponds to a transverse mode, i.e., a field enhancement along the short axis. Hence, UV light acts as feedback irradiation: if a particle starts to grow flat, the UV photoreduction process makes the particle grow back as a sphere. This is clearly observed on the absorption spectrum of the UV-irradiated synthesis (Figure 5A) where particles exhibit a strong peak at 420 nm with a shoulder at 350 nm, corresponding to either large spherical particles or flat particles with an aspect ratio very close to 1.

Irradiation wavelength dependency is well illustrated by regrowth experiments in Figure 5B. A solution of nanodisks obtained after 90 min of irradiation at 457 nm was used as seed and further irradiated in the presence of additional citrate and silver nitrate with the same concentration as in the initial experiment. When particles were further irradiated at the same wavelength, 457 nm, their size increased but the longitudinal plasmon band remained at the same position, indicating a constant aspect ratio. However, if particles were irradiated at 514 nm the in-plane band shifted to 615 nm, indicating a larger aspect ratio. As they grow in size, their aspect ratio varies with the irradiation wavelength.

Conclusion and Discussion. Silver nanoparticles were grown by irradiating a sample of silver nanoparticle seeds, silver ions, and citrate with a laser. Citrate serves as a reducing agent and as a capping ligand for the silver nanoparticles; silver ions are reduced on the surface of the nanoparticles. The concentration of silver ions in solution controls the final size of the particles. The aspect ratio is controlled by the irradiation wavelength (i.e., the longer the wavelength, the larger the aspect ratio) due to the shape dependence of the Ag plasmon resonance. This controlled growth mechanism might be used in the future to directionally grow fixed particles on a surface and to controllably narrow a junction between two Ag electrodes.

Our results on the wavelength dependence of aspect ratio are similar to those observed in the nanoparticle-to-nanoprisms photoreformulation experiment (without added Ag ion and reducing agent) of Mirkin et al.¹⁷ We suggest that in their experiment, some silver ions were present in equilibrium with reduced silver in the particles.²⁷ This Ostwald dissolution of silver ion into solution will be enhanced by dissolved oxygen which raises the particle redox potential.²⁸ The photoreformulation process is driven by room lights and takes about 50 h to be completed, a reasonable result in view of the low quantum yield we find and the slow dissolution process.

Acknowledgment. We thank Chad Mirkin for an informative discussion of ideas and unpublished results and Arnim Henglein for constructive comments on this manuscript. We also thank Alexander Hallock and Peter Redmond for discussions and comments. This work has been supported by DOE Basic Energy Science under FG02-98ER14861. Undergraduate REU student P. Huang was supported by the EMSI environmental program under CHE-98-10367. We have used materials characterization facilities supported by the Columbia-CCNY MRSEC under DMR 02123547.

References

- (1) Michaels, A. M.; Nirmal, M.; Brus, L. E. *J. Am. Chem. Soc.* **1999**, *121*(43), 9932–9939.
- (2) Nie, S.; Emory, S. R. *Science* **1997**, *275*, 1102–1106.
- (3) Kneipp, K.; Wang, Y.; Kneipp, H.; Perelman, L. T.; Itzkan, I.; Dasari, R.; Feld, M. S. *Phys. Rev. Lett.* **1997**, *78*, 1667.
- (4) Xu, H. X.; Bjerneld, E. J.; Kall, M.; Borjesson, L. *Phys. Rev. Lett.* **1999**, *83*, 4357.
- (5) Weiss, A.; Haran, G. *J. Phys. Chem. B* **2001**, *105*, 12348.
- (6) Maier, S. A.; Kik, P. G.; Atwater, H. A.; Meltzer, S.; Harel, E.; Koel, B. E.; Requicha, A. A. G. *Nature Materials* **2003**, *2*, 229–232.

- (7) Zanchet, D.; Micheel, C. M.; Parak, W. J.; Gerion, D.; Williams, S. C.; Alivisatos, A. P. *J. Phys. Chem. B* **2002**, *106*, 11758–11763.
- (8) Jin, R.; Wu, G.; Li, Z.; Mirkin, C. A.; Schatz, G. C. *J. Am. Chem. Soc.* **2003**, *125*(6), 1643–1654.
- (9) Linnert, T.; Mulvaney, P.; Henglein, A. *Ber. Bunsen-Ges. Phys. Chem.* **1991**, *95*(7), 838–841.
- (10) Henglein, A.; Giersig, M. *J. Phys. Chem. B* **1999**, *103*, 9533–9539.
- (11) Mulvaney, P.; Giersig, M.; Henglein, A. *J. Phys. Chem.* **1992**, *96*, 10419–10424.
- (12) Ahern, A. M.; Garrell, R. L. *Anal. Chem.* **1987**, *59*(23), 2813–2816.
- (13) Bjerneld, E. J.; Murty, K. V. G. K.; Prikulis, J.; Kall, M. *ChemPhysChem* **2002**, *1*, 116–119.
- (14) Turkevitch, J.; Stevenson, P. L.; Hillier, J. *J. Discuss. Faraday Soc.* **1951**, *11*, 55.
- (15) Chen, S.; Fan, Z.; Carroll, D. L. *J. Phys. Chem. B* **2002**, *106*(42), 10777.
- (16) Pastoriza-Santos, I.; Liz-Marzan, L. M. *Nano Lett.* **2002**, *2*(8), 903.
- (17) Jin, R.; Cao, Y.; Mirkin, C. A.; Kelly, K. L.; Schatz, G. C.; Zheng, J. G. *Science* **2001**, *294*, 1901.
- (18) Maillard, M.; Giorgio, S.; Pileni, M. P. *Adv. Mater.* **2002**, *14*, 1084.
- (19) Sun, Y.; Xia, Y. *Adv. Mater.* **2003**, *15*, 695.
- (20) Germain, V.; Li, J.; Ingert, D.; Wang, Z. L.; Pileni, M. P. *J. Phys. Chem. B* **2003**, *107*(34), 8717–8720.
- (21) Kreibig, U.; Vollmer, M.; *Optical Properties of Metal Clusters*; Springer: Berlin, 1993.
- (22) Taking into account that initial particles are small (8 nm), it is assumed that scattering does not contribute significantly to the nanoparticle's extinction coefficient. Hence, absorbance and extinction coefficient are equal, in first approximation.
- (23) Munro, C. H.; Smith, W. E.; Garner, M.; Clarkson, J.; White, P. C. *Langmuir* **1995**, *11*, 3712–3720.
- (24) Sato, T.; Kuroda, S.; Yonezawa, Y.; Hada, H. *Appl. Organometallic Chem.* **1991**, *5*, 261–268.
- (25) Rogach, A. L.; Shevchenko, G. P.; Afanaseva, Z. M.; Sviridov, V. V. *J. Phys. Chem. B* **1997**, *101*, 8129–8132.
- (26) Chen, C. J.; Osgood, R. M. *Phys. Rev. Lett.* **1983**, *50*, 1705.
- (27) Silvert, P.-Y.; Herrera-Urbina, R.; Tekaia-Elhsissen, K. *J. Mater. Chem.* **1997**, *7*(2), 293–299.
- (28) Henglein, A. *Chem. Mater.* **1998**, *10*, 444–450.

NL034666D